Sprayed single phase $CuIn_{0.6}Ga_{0.4}S$ thin films for solar cell applications; Solvent-dependent growth

FAWZY A. MAHMOUD[*a, b] A.Y. ELIWA[*c], NINET AHMED[c], WAFAA MAGDY[a,b]
[a]*Solid State Physics Dept., National Research Center, P.O. 12311, Dokki, Giza, Egypt*
[b]*Solar cell lab., Center of Excellence for Advanced Sciences, National Research Centre, P.O.12311, Dokki, Giza, Egypt*
[c]*Photovoltaic department, Electronics Research Institute, Dokki, Giza, Egypt*

Single phase copper indium gallium sulfide (CIGS) thin films were deposited on a glass substrate by spray pyrolysis technique. Three spray solutions, were prepared with different solution solvents; Ethyl alcohol, Ethylene glycol and 2-Ethoxyethanol. The effect of solvent type on the structural, electrical, optical and surface properties has been investigated. XRD reveals the polycrystalline nature of CIGS films and predominate of (112) plane for all prepared films. Optical investigation showed that the value of absorption coefficient is in the order of 10^5 cm^{-1}, indicating direct allowed energy gap about 1.5 eV. Thin film prepared using Ethyl alcohol solvent showed better crystallinity with a bigger crystallite size and lowest resistivity of 3.7×10^{-1} Ω.cm. Three solar cells based on prepared samples with CIGS/n-Si structure was constructed and their I-V curves were measured. We found that the cell fabricated from Ethyl alcohol based spray solution shows the better I-V curve.

(Received February 03, 2016; accepted April 05, 2016))

Keyword: Single phase *CuIn0.6Ga0.4S,* Thin film, Spray pyrolysis, Solar cells

1. Introduction

Solar cells based on more simple structures are promising for solar energy conversion due to their relatively low production cost. Therefore, thin film materials with higher absorption coefficient have been strongly explored like amorphous Si thin film, chalcogenide based materials and Cadmium-Telluride [1]. Chalcopyrite semiconductors have attracted widespread attention for use in thin-film solar cells. Solar cell technologies using I-III-VI2 chalcopyrite semiconductors have made rapid progress in recent years [2-3]. Conversion efficiencies for polycrystalline CIGS based solar cells have been significantly improved over recent years and the best cell have achieved at 19.9 % up to now [4]. CIGS compound solar cell has been aggressively investigated because this p-type semiconductor has desirable properties such as high optical absorption coefficient in the range of 10^5 cm^{-1} in the visible region with a near-optimum band gap of 1.5 eV [5], which have been considered the most promising alternative to crystalline silicon solar cells [1]. Within the copper based family of chalcopyrite semiconductors, the sulfur compounds, such as $CuInS_2$, $CuGaS_2$ and $CuInGaS_2$, have been gaining more attention due to no need for selenium containing toxic precursor materials [6-10]. However, there are very limited studies on wet chemical deposition of the $CuInGaS_2$ thin films [11–14]. Up to now $CuInGaS_2$ based solar cells have lower efficiencies in comparison to the corresponding $CuInGaSe_2$. This is mainly caused by too low open circuit voltages (V_{OC}) of these solar cells in relation to the band gap energy of the absorber material [18].

CIGS thin films have been grown using a variety of deposition techniques, such as electrodeposition [19], spray pyrolysis [20], two-step process [21], sputtering [18,22], evaporation [23], sonochemically [24], hot-injection method [25].

It is well known that widespread use of solar cells will only be possible if non-toxic materials are used and if a fast, inexpensive and scalable technique is available for the deposition. Spray pyrolysis could fulfill these requirements, providing films with optical and electrical properties comparable with those grown by the more expensive vacuum deposition techniques currently used [26]. It is evident that the solvent used in the spraying process has an important role in determining the properties of the film since solvent vaporization and thermal decomposition of precursor solutes significantly affect material properties [27]. The use of solvents with different points of boiling and viscosity aimed at the optimization of operating parameters to obtain homogeneous and dense CIGS film

Few reports have been devoted to study of the influence of solvent upon film properties [20]. However, no comparative study of the structural, optical and electrical properties of CIGS thin film samples prepared using different solvents of CIGS spraying solutions is reported. In this work, we studied the role of the solvent type in a spray solution on the structural, optical and electrical properties of CIGS thin films.

Three different types of precursor solutions, based on solvent type, were used for the film preparation. The boiling points and viscosity of the three solvents; Ethyl alcohol, Ethylene glycol and 2-Ethoxyethanol are; 78.37 ^{o}C and 1.2 CP [28], 197.6 ^{o}C and 16.9 CP [29], 135 ^{o}C and

2.5 CP [30-31] respectively. The effect of solvent on the structure, optical and electrical characteristics was investigated to optimize the sprayed CIGS absorber thin film for thin film solar cell applications. Finally, we prepared three samples of p- CIGS /n-Si heterojunction (HJ) solar cells by spray pyrolysis technique.

2. Materials and methods

Three different samples from CIGS thin film were prepared by a spray pyrolysis technique based on three different solution solvents**;** Ethyl alcohol, Ethylene glycol and 2-Ethoxyethanol. The precursor solutions were prepared using 0.1M of $CuCl_2:2H_2O$ (Sigma-Aldrich), 0.1M of $InCl_3:4H_2O$ (Aldrich, 98%), 0.1M of $Ga(NO_3)_3\cdot xH_2O$ (Aldrich, 99.9%) and 0.1M of $SC(NH_2)_2$ (Sigma-Aldrich, 99.00%) dissolved in three different solvents: Ethyl alcohol, Ethylene glycol and 2-Ethoxyethanol for preparing three different spray solutions. Solution concentration of 0.1M is sprayed onto ultrasonically cleaned preheated glass substrate maintained at 400^{o} C using temperature controller with an accuracy of±5 ◦C. Compressed filtered air was used as the carrier gas with a flow rate of 20 L/ min. The solution flow rate was kept at 2 mL/ min. The distance between the nozzle and the substrate was maintained at 30 cm. The Cu: In: Ga: S ratio in the solution was maintained at 1:0.6:0.4:1. The structural properties of CIGS thin films were studied by computer controlled X-ray diffractometer (PANalytical Empyrean) with Cu kα- radiation (λ= 1.5406 Å) operated at 30 mA and 45 kV. The data were collected at room temperature in step scanning mode, the 2 range of 20–90°, with scan step 0.02, counting time 20s/step and grazing angle 1.5° of incident X-rays. The surface morphology of the films was examined by Scanning Electron Microscope (SEM); FEI Quantum FEG 250. The thickness of films was measured using Dektak 150 Stylus profilmeter. Energy dispersive X-ray analysis (EDX) was determined by JEOL (JXA-840A) electron probe microanalyzer which utilized to examine the composition of the films. The optical properties were obtained by UV/Vis/NIR spectrophotometer model Jasco-670 in the wavelength range 200–2500 nm. The resistivity measurement of the deposited films was carried out using 'two probe method' performed with Keithley 2110 computerized digital multimeter at different temperatures. Current-Voltage (I-V) measurements of the $p\text{-}CIGS_2/n\text{-}Si$ solar cells were performed using Photo Emission Tech. INC I-V Test System under illumination of 100 mW/cm^2 at 25 ^{o}C.

3. Results and discussion

3.1 Structural properties

Well adherent, pinhole free, uniform dark brown colored films of CIGS were formed on the surface of substrates. Figure 1 shows XRD patterns for the CIGS films prepared from three solvents; Ethyl alcohol, Ethylene glycol and 2-Ethoxyethanol. X-ray diffraction studies revealed that all films are polycrystalline CIGS phase with crystalline chalcopyrite structure and predominantly (112) oriented films, irrespective of solvent type. X-ray diffraction patterns show three main peaks at 2θ of 28.14, 46.28, and 56.70; these peaks were indexed by JSPDS Cards no; 00-056-1309 at (112), (220) and (132) respectively that related to $CuIn_{0.6}Ga_{0.4}S$ phase [17]. Also, we can see other peaks with low intensities that related also to the same phase. Hence the intensity of (112) plane may have a clear dependence on the type of the solvent used in the precursor solution. Also the XRD data showed that (112) peak related to the film prepared using ethyl alcohol has higher intensity than films prepared using other two solvents which means higher crystallinity; this can be attributed to different volatility between three solutions which can be attributed to the low boiling point of ethyl alcohol.

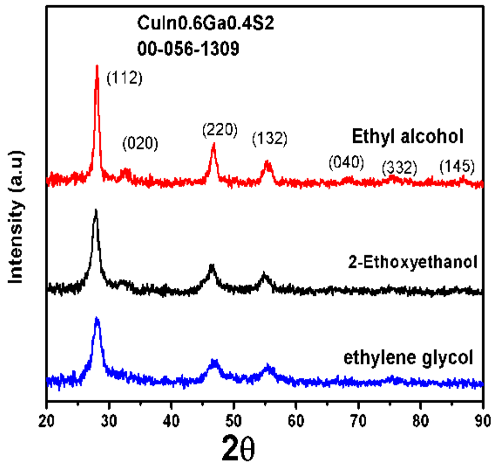

Fig.1 XRD of CIGS thin films deposited at 30 min. and 400 °C using 3 different solvents

The crystallite size is estimated from full width at half maximum (FWHM) of main diffraction peak (112) using Scherer's formula [15].

$$D = \frac{k\lambda}{\beta \cos\theta} \quad (1)$$

Where, D is the crystallite size, k is a constant taken to be 0.94, β is the full width at half maximum (FWHM) and λ is the wave length of the x-rays (1.54178Å**)**. The calculated crystallite size corresponding to (112) preferred orientation of crystalline thin films prepared from different solvents; Ethyl alcohol, 2-Ethoxyethanol and Ethylene glycol are 14.77 nm, 5.52 nm and 5.28 nm respectively. It is observed that, the crystallite size of the $CuIn_{0.4}Ga_{06}S$ film prepared with ethyl alcohol is larger than those prepared with other two solvents. This may be due to the difference in the boiling points and viscosity of the three solvents used in this work resulting in the 'residence time' of the droplets on the hot substrate and consequently in thin film formation mechanism. In other words, this result may be due to the low viscosity and boiling points of ethyl alcohol than other solvents [32-33].

3.2 SEM

Fig. 2 describes SEM micrographs of the prepared films with different solvents at 400 °C. The morphology of prepared films indicated that the films are made of almost uniform crystallites. The analysis of SEM micrographs clears that, the surface nature of the films is greatly influenced by the variation of the precursor solution solvent. Different atomic rearrangement processes involved during the pyrolytic decomposition of the sprayed droplets onto the hot substrates are responsible for the difference in observed surface topography of the CIGS films.It is observed that the sample prepared using Ethyl alcohol solvent shows better morphology with well-faceted and compact grains with some cracks as compared with samples prepared using Ethylene glycol and 2-Ethoxyethanol solvents. CIGS layer prepared using Ethyl alcohol has bigger crystallite sizes since this solvent has a lower boiling temperature, leading to faster vaporization and crystalline with smooth shape [33].

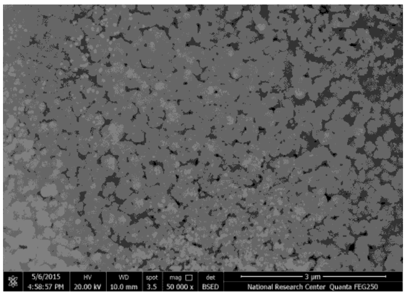

Ethyl Alcohol

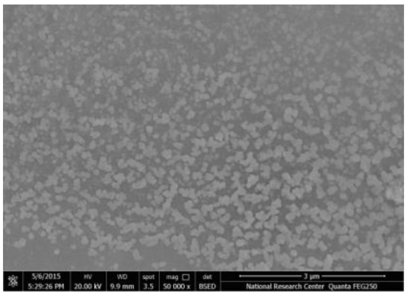

2-EThoxyEthanol

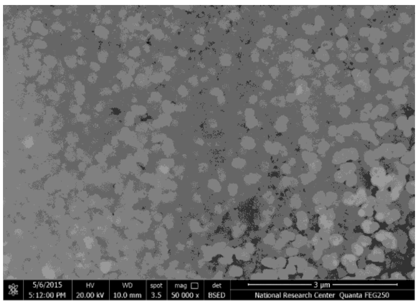

Ethylene glycol

Fig.2 SEM images of CIGS thin films deposited at 400 ^{o}C using 3 different solvents

3.3 EDAX

Energy dispersive X-ray (EDX) microanalysis has been used to evaluate the chemical compositions of the films. Figure 3 shows the EDX spectra of the CIGS films prepared at a substrate temperature of 400 ^{o}C using Ethyl alcohol. EDX spectra of the films were taken to see whether Cu, In, Ga and S elements in the starting solutions are present in the solid films or not. Table 1 summarizes the atomic weight of the four elements Cu, In, Ga and S of CIGS films prepared with three different spray solutions solvents. We can see that the sample, prepared with ethyl alcohol as solvent, shows better stoichiometry and low impurities than other samples. Ethyl alcohol was expected to yield the lowest impurity content because of its low carbon and oxygen content [33].

In addition, ethyl alcohol had the lowest boiling point, which in turn facilitated evaporation of the solvent. Also, Si, Ca and Na elements are present in the solid films. It is

Table 1. Elemental analysis data of CIGS thin film prepared from different solvents.

Element Solvent	Cu %	In %	Ga %	S %
Ethyl alcohol	33.57	10.51	10.84	45.08
2-Ethoxyethanol	27.23	9.99	18.64	44.14
Ethylene glycol	25.55	12.09	13.33	49.04

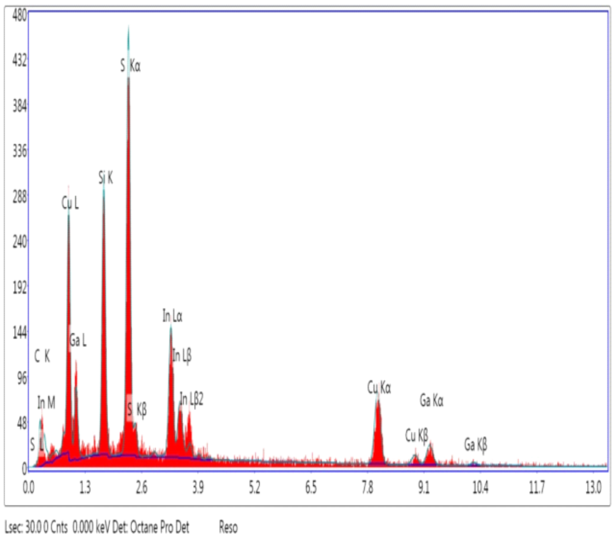

Fig. 3. EDX spectra of CIGS thin films deposited at 400 ^{o}C using Ethyl alcohol solvent

3.4 Optical properties

The variation of transmittance with wavelength for films deposited from different solvents are shown in figures 4. As seen in Fig. 4, transmittance spectra are sharp increases in the range of about 750 nm which indicate to the good crystallinity of our prepared samples where the best crystalline film. Ethyl alcohol based sample has a sharp edge than the others where this sample crystalline is better than the others. The transmittance of the films is negligible in visible region which indicates that the films are highly absorbing in this region [34]. Also from Fig.4, it is clear that the sample with Ethyl alcohol solvent has a maximum transmittance in the NIR region compared to the samples prepared with other solvents samples.

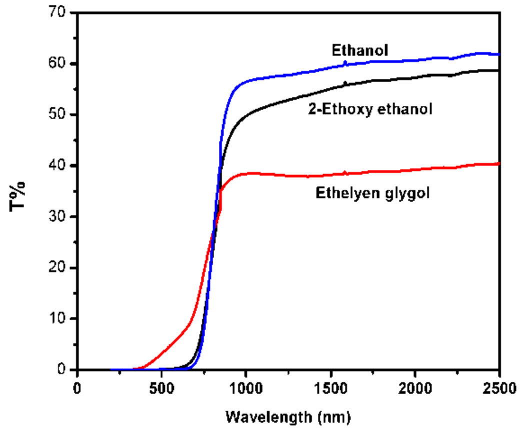

Fig. 4. Optical transmittance spectra of CIGS thin film versus wavelength for films deposited from different solvents.

3.4.1 Absorption coefficients

Fig. 5 shows the absorption coefficient versus wavelength plots for the CIGS films for the different solvents. The absorption coefficient was calculated from transmittance values using the following expression [34]:

$$\alpha = \frac{1}{t}\ln\left(\frac{1}{T}\right) \tag{2}$$

Where, α is the absorption coefficient, T is the transmittance values and t is the thickness of the film. The films have a high optical absorption coefficient over than 1 $\times 10^5$ cm^{-1}, which is in good agreement with other reports in the literature [21].

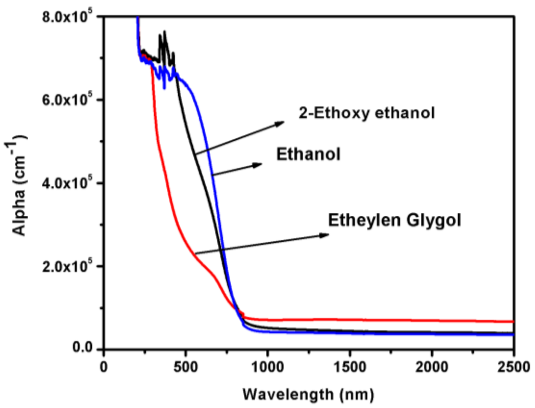

Fig. 5. Absorbance coefficient of CIGS thin film versus wavelength for films deposited from different solvents.

3.4.2 Energy gap

The variation of $(\alpha h\nu)^2$ versus photon energy (hν) is shown in Fig. 6. The bandgap energy E_g was estimated from the plots of $(\alpha h\nu)^2$ against (hν) according to the following equation [11]:

$$(\alpha h\nu)^2 = A(E_g - h\nu) \tag{3}$$

Where A is a constant, α is the absorption coefficient, h is Planck's constant and ν is the frequency of the photon. The extrapolation of this curve to zero absorption coefficient (i.e. α = 0) gives the bandgap energy. Band gap values of CIGS films have been determined to be 1.53, 1.53 and 1.56 eV for Ethyl alcohol, 2-Ethoxyethanol and Ethylene glycol respectively. This is close to the optimal bandgap required for solar cells and therefore these films are considered to be suitable for use as an absorbent material for photovoltaic applications. It is observed that, band gaps of films do not change drastically by changing the solvent type.

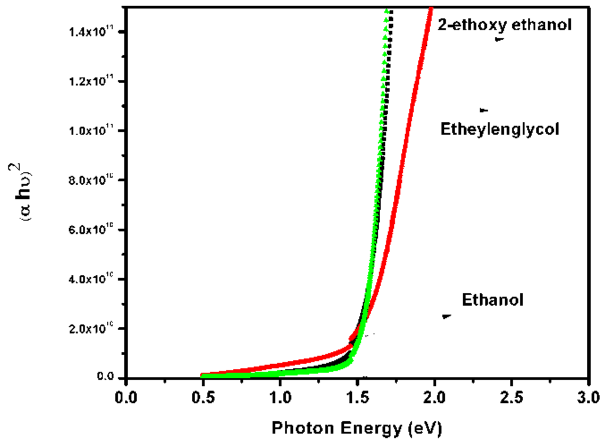

Fig.6. Plot of $(\alpha h\upsilon)^2$ versus hυ for CIGS thin films deposited from different solvents.

3.4.3 Refractive index

The refractive index versus the wavelength of the deposited CIGS thin films is shown in Fig. 7. The refractive index was calculated from reflectance data using the following expression [35]:

$$n = \frac{(1 + R^{1/2})}{(1 - R^{1/2})} \tag{4}$$

The minimum value of refractive index is 1.29 in the visible region reported for Ethyl alcohol, which is suitable to use as an absorbent material of solar cells without antireflection layer.

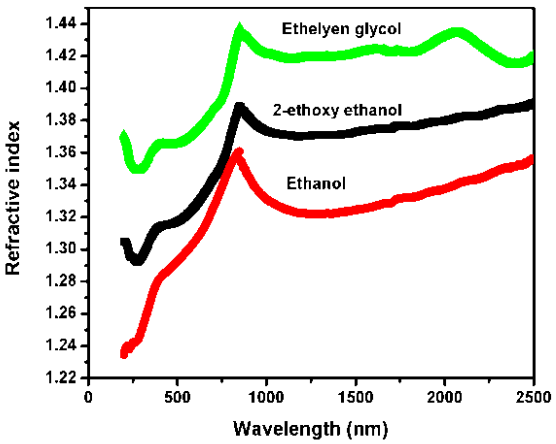

Fig. 7. Refractive index of CIGS thin film versus wavelength for films deposited from different solvents.

Table 2. Some optical parameters of CIGS thin film versus wavelength for films deposited from different solvents

Solvent Type	α(cm^{-1})	Eg (eV)	Refractive Index (n)
Ethyl alcohol	$6x10^5$	1.53	1.29
2-Ethoxyethanol	$6x10^5$	1.53	1.32
Ethylene glycol	2.2×10^5	1.56	1.36

3.5 Electrical properties

All prepared CIGS thin films exhibit p-type conductivity. The temperature dependence of electrical conductivity of CIGS films was measured in the temperature range of 300–500 K. Figure 8 shows the variation of the dark conductivity (lnσ) with the reciprocal temperature 1/T. From this figure, it is seen that dark conductivity increases linearly with increasing temperature indicating the semiconducting behavior of the CIGS films. Also, this figure indicates that, films prepared using ethyl alcohol has the maximum conductivity on the order of 2.7 $\Omega^{-1}cm^{-1}$. The electrical conductivity is higher for CIGS sample obtained using ethyl alcohol; due to the maximum crystallite size associated with this solvent and conductive Cu-rich phases segregated on the surface and results on low resistivity. This data is further used to determine the activation energy by using the following relation [36].

$$\sigma = \sigma_o \exp(\frac{-E_a}{KT}) \quad (5)$$

Where, σ_o is a pre-exponential factor, K is the Boltzmann constant, E_a is the thermal activation energy. From the slope of this graph the activation energy is estimated. The activation energy of the Ethyl alcohol CIGS sample is equal to 0.0716 eV which is the lower activation energy as compared to others. Table 2 indicates the activation energy and the optical band gap for $CuIn_{0.6}Ga_{0.4}S$ thin films. Table 3 is summarized some of structural and electrical properties of $CuIn_{0.6}Ga_{0.4}S$ thin films.

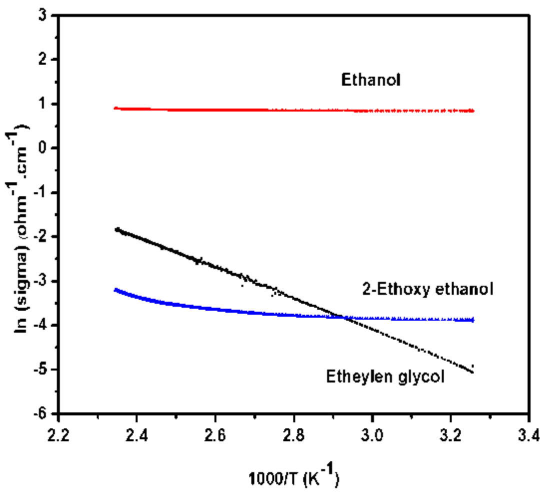

Fig. 8. Variation of electrical conductivity with reciprocal temperature for the three selected solvent.

Table 3. Some structural and electrical properties of $CuIn_{0.6}Ga_{0.4}S$ thin film and also the photovoltaic parameters of p-CIGS/n-Si heterojunction solar cells.

Type of Solvent	Grain size (nm)	Electrical properties		photovoltaic parameters of p-CIGS/n-Si heterojunction solar cells			
	Plane of calculation (112)	σ $(\Omega cm)^{-1}$	Ea (eV)	Voc (mV)	Isc A	FF	η (%)
Ethyl alcohol	14.77	2.7	0.0716	150	$1 x10^{-6}$	0.6	0.00009
2-Ethoxyethanol	5.52	0.0111	0.1625	125	$6x10^{-7}$	0.4	0.00003
Ethylene glycol	5.28	0.00673	0.301	80	$1.4x10^{-7}$	0.3	0.0000034

4. Solar cells

Three samples of P-CIGS/n-Si heterojunction solar cell using three different solvents are prepared by chemically spray P-CIGS on n-type (111) single crystal silicon wafers. The resistivity and thickness of silicon wafers were 1-5 Ωcm and 300 μm respectively. Prior to deposition of CIGS films, these wafers were chemically etched in dilute hydrofluoric acid and then washed with de-ionized water to remove the native oxide. They were, finally, ultrasonically cleaned using isopropyl alcohol. Subsequently, after oxide removing, the wafers were scribed into individual pieces of area 1 cm^2, and then they were exposed to spraying CIGS film to obtain the p-CIGS/n-Si heterojunction. Metallization ohmic electrodes were accomplished using vacuum evaporation to deposit Ag onto the entire back of the Si substrate and a front grid through a metal mask on the CIGS surface. Photovoltaic properties of the samples prepared with CIGS films based on different solvents are investigated. Table 3 indicates the photovoltaic parameters of the three samples, I-V characteristics of the three p-CIGS/n-Si samples show poor photovoltaic response. The conversion efficiencies of the three p-$CIGS_2$/n-Si cells are small (< 1%). This was most probably due to the high series resistance which may be attributed to the ohmic contacts. It is observed that, the best photovoltaic response obtained for the sample deposited from the sprayed solution using Ethyl alcohol. This may be attributed to the better structural, optical and electrical properties of this CIGS film than the two others. These results on relatively low series resistance, thus leading relatively to larger short-circuit current density. Figure 9 shows the illuminated I-V characteristics of p-$CIGS_2$/n-Si cell sample fabricated using Ethyl alcohol. The effect of gallium replacement with indium on physical properties of sprayed $CuIn_{1-x}Ga_xS_2$ films prepared using Ethyl alcohol for a precursor solution will be investigated in the next study. Also, CdS/ CIGS solar cell based on optimum $CuIn_{1-x}Ga_xS$ film using molybdenum as an electrode for the CIGS layer will be constructed and characterized.

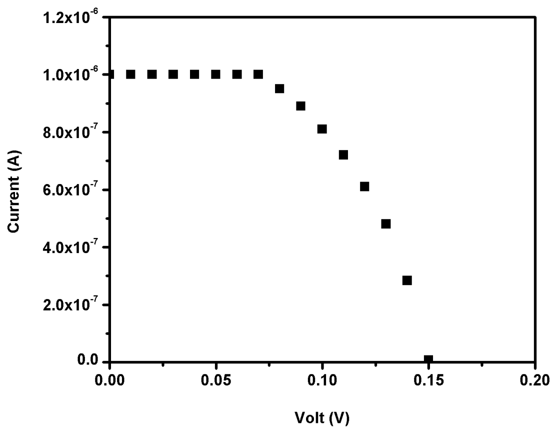

Fig. 9. Illuminated I-V characteristics of p/CIGS/n-Si solar cell deposited using Ethyl alcohol.

5. Conclusion

Single phase copper indium gallium sulfide (CIGS) thin films, in one step, were prepared on a glass substrate by spray pyrolysis technique. we investigated the effect of solvent on the properties of spray pyrolysis CIGS thin film. Three different precursors were studied; Ethyl alcohol, 2-Ethoxyethanol and Ethylene glycol. XRD spectra indicate that, all films exhibit crystalline chalcopyrite structure with preferred orientation growth along (112) plane. The preferred growth plan remained predominant irrespective of the solvent. The best crystallinity is obtained from Ethyl alcohol since the maximum (112) peak intensity and grain size are obtained using this solvent. EDAX spectra of CIGS films identify Cu, In, Ga and S elements for all solvents. Band gaps of synthesized layer corresponding to the three solvents are 1.53, 1.53 and 1.56 eV, which is suitable as an absorbent layer in efficient thin film solar cells. Also, the higher Cu concentrations obtained single chalcopyrite phase with bigger grains is the most suitable for solar cell applications. We found that the best electrical properties have been obtained for the CIGS thin films prepared by using Ethyl alcohol. Also, the best photovoltaic response obtained for the sample deposited using the sprayed solution of this solvent. This can be attributed to the low vicousty of Ethyl alcohol because high viscosity solvents contain impurities (i.e., Cl, O, C, N, and Na) that add resistance and degrade solar cell performance.

References

[1] Chulwon Chung, Dongjoon Rhee, Dongjun Yoo, Moonsuk Choi, Seung Chan Heo, Dohyung Kim, Changhwan Choi, Journal of Ceramic Processing Research. **14**(2), 255 (2013).
[2] Sh. M. Ebrahim, I. Morsi1, M. M. Soliman , M. Alshrkawy1 , A. A. Elzaem, International Conference on Control, Automation and Systems 2010 Oct. 27-30, 2010 in KINTEX, Gyeonggi-do, Korea.
[3] B. J. Babu, S. Velumani, Arturo Morales-Aceedo, R. Asomoza, 2010 7th International Conference on Electrical Engineering, Computing Science and Automatic Control (CCE 2010), Tuxtla Gutiérrez, Chiapas, México, September 8-10, p. 581 (2010).
[4] S. Parag Vasekar, G. Neelkanth Dhere, Solar Energy Materials & Solar Cells, **93,** 69 (2009).
[5] P. Chelvanathan, M. Istiaque Hossain, N. Amin, Current Applied Physics **10**, S387 (2010).
[6] S. Gall, N. Barreau, S. Harel, J.C. Berne`de, J. Kessler, Thin Solid Films, **480–481**, 138 (2005).
[7] Se Jin Park, Jin Woo Cho, Joong Kee Lee, Keeshik Shin, Ji-Hyun Kim and Byoung Koun Min, Prog. Photovolt: Res. Appl., **22**, 122 (2014).
[8] A.Romeo, M. Terheggen, D. Abou-Ras, D. L. Ba¨tzner, F.-J. Haug, M. Ka¨lin, D. Rudmann1, A. N. Tiwari Prog. Photovolt: Res. Appl., 93 (2004).

[9] M. Kaelin, D. Rudmann, A.N. Tiwari, Solar Energy, 77(6), 749 (2004).
[10] Parag S. Vasekar, Anant H. Jahagirdar, Neelkanth G. Dhere, Thin Solid Films, **518**, 1788 (2010).
[11] Mejda Ajili, Michel Castagné, Najoua Kamoun Turki, Journal of Luminescence, **150**, 1 (2014).
[12] H. Anant Jahagirdar, G. Neelkanth Dhere, Solar Energy Materials & Solar Cells, **91**, 1488 (2007).
[13] P. Jitendra Sawanta, B. Rohidas Kaleb, International Journal of Engineering Research and General Science, **3**(2), 533 (2015).
[14] H.-C. Jin Michael, K. Kulbinder Banger, D. Jerry Harri, F. Aloysius Hepp, Materials Science and Engineering B 116, 395 (2005).
[15] P. M. Parameshwari, Shashidhara Bhat, K. Gopalakrishna Naik, Archives of Physics Research, **3(**6), 441 (2012).
[16] N. Demirci Sankir, E. Aydin, E. Ugur, M. Sankir, Journal of Alloys and Compounds, **640**, 468 (2015).
[17] S. Liu, L. Nie, R. Yuan, Chalcogenide Letters, **12**(3), 111 (2015).
[18] J. Reck, S. Seeger, M.Weise, R. Mientus, J. Schulte, K. Ellmer, Thin Solid Films, **571**, 762 (2014).
[19] S. Merdes, D. Abou-Ras, R. Mainz, R. Klenk, M. Ch. Lux-Steiner, A. Meeder, H. W. Schock, J. Klaer, progress in Photovoltaics: Research and Applications, **21**(1), 88 (2013).
[20] E. Aydin, M. Sankir, N. Demirci Sankir, Journal of Alloys and Compounds, **615**, 461 (2014).
[21] R. Mainz, J. Klaer, R. Klenk, N. Papathanasiou, 22nd European Photovoltaic Solar Energy Conference, 3-7 September 2007, Milan, Italy, p. 2429.
[22] M. Nie, K. Ellmer, Thin Solid Films, **536**, 172 (2013).
[23] R. Kaigawa, A. Neisserb R. Klenk, M.-Ch. Lux-Steiner, Thin Solid Films **415**, 266 (2002). Acta Physica Polonica A, **126**(5), 1107 (2014).
[25] Duy-Cuong Nguyen, Ken Fukatsu, Keiji Tanimoto, Shigeru Ikeda, Michio Matsumura, Seigo Ito, Hindawi Publishing Corporation, International Journal of Photoenergy, (2013), Article ID 416245,
[26] E. Arca, K. Fleischer, I.V. Shvets, Thin Solid Films, **520**, 1856 (2012).
[27] T. V. Vimalkumar, N. Poornima, C. Sudha Kartha, K.P. Vijayakumar, Materials Science and EngineeringB, **175**, 29 (2010).
[28]http://www.dow.com/ethylalcohol/about/properties.htm.
[29]http://www.dow.com/ethyleneglycol/about/properties.htm.
[30] https://en.wikipedia.org/wiki/2-Ethoxyethanol.
[31]http://www.stenutz.eu/chem/solv6.php?name=2-ethoxyethanol.
[32] Ji Hoon Woo, Hyun Yoon, Ji Hyun Cha, Duk Young Jung Sam S. Yoon, Journal of Aerosol Science, **54**, 1 (2012).
[33] S. Benramache, A. Rahal, B. Benhaoua, Optik, **125**, 663 (2014).
[34] G. Muruganantham, K.Ravichandran, S. Sriram, B. Sakthivel, J. Optoelectron. Adv. Mat. **14(**3-4), 277 (2012).
[35] M. David Femi, A. Ohwofosirai, A. Sunday, O. Sunday, B. A. Ezekoye, F. I. Ezema, R. U. Osuji, International Journal of Advances in Electrical and Electronics Engineering, **2**(2), p. 331.
[36] S. Mammen, C.S. Menon, N.V. Unnikrishnan, Materials Science-Poland, **23**(3), 707 (2005).

*Corresponding author: fawzyhameed@yahoo.com
fa.mahmoud@nrc.sci.eg
aref@eri.sci.eg